

Growth Animation of Human Organs

Roman Ďurikovič Silvester Czanner *;
Hirofumi Inoue

Computer Graphics Laboratory, Software Department, The University of Aizu,
Ikki-machi, Aizuwakamatsu-shi, Fukushima, 965 8580 Japan.

Tel.: +81-242-37-2641, Fax: +81-242-37-2706
email: roman,czanner@u-aizu.ac.jp

Abstract

The growth of the organs of human embryo is changing significantly over a short period of time in the mother body. The shape of the human organs is organic and has many folds that are difficult to model or animate with conventional techniques. Convolution surface and function representation are a good choice in modelling such organs as human embryo stomach and brain. Two approaches are proposed for animating the organ growth: First, uses a simple line segment skeleton demonstrated on a stomach model and the other method uses a tubular skeleton calculated automatically from a 2D object outline. The growth speed varies with the position within the organ and thus the model is divided into multiple geometric primitives that are later glued by a blending operation. Animation of both the embryo stomach and brain organs is shown.

Keywords: geometric modelling, skeleton, blending operation, convolution surface.

1 Introduction

Human organs during their development can undergo significant changes in shape through a variety of global transformations, such as bending or twisting. Because, it is very difficult to see and to understand growth process of organs the embryologists found the realistic models of human organs and animations of their shape changes during the growth necessary in their studies. Biological organ grows nonlinearly and yet obeys certain rules.

The purpose of this manuscript is to model the outer shape and the shape metamorphosis during the growth

*On leave from Department of Computer Graphics and Image Processing, Faculty of Mathematics, Physics and Computer Science, Comenius University, Bratislava, Slovakia

of some human embryo organs, particularly brain and stomach. Popular methods like 3D shape reconstruction from Computer Comography (CT) sections or ultrasound data can not be used for this type of modelling because the resolution of the devices used in those methods are much higher comparing to the size of human embryo. Four weeks old embryo is approximately 3 mm tall while the CT resolution is 1 mm giving us only three sections for a reconstruction process. Usually, the microscopic cross-sections are used to reconstruct the polygonal representation of an embryo, which is exact but complicated process. In case of such destructive approach often a mouse embryo is used instead of the human embryo.¹³ To control the shape metamorphosis between two mesh objects become a problem when they have different topology and geometry. To create the realistically looking human organ models and to generate the animations demonstrating the growth process requires an appropriate methodology. The aim of this paper is to present a methodology based on the functional representation and convolution surfaces.^{1,10}

S. Muraki⁷ use implicit iso-surfaces generated by a number of field generating primitives, so called *Blobbe Model*, for shape reconstruction from the range data. An initial point skeleton is placed at the center of mass of the range data points. A correct approximation is found by energy minimization problem, the result is a set of point skeletons and optimal *Blobby* parameters. The problem of this method is that the final shape can be topologically discontinuous i.e. the artifacts occur. This is partially solved by N. Tsingos *et al.*¹² proposed a semi-automatic geometrical representation of organs using the implicit surfaces, the user initially position some skeleton points, and further optimize the process by specifying the *reconstruction windows*. The result of the optimization is discontinuous skeleton consisting of a set of discrete points. Slight overlapping of

reconstruction windows can avoid the topology discontinuity, but there is no guarantee the particular shape in each *reconstruction window* has no topological artifacts.

The method developed by Attali *et al.*² computes the Voronoi graph of the point set to build the skeleton of the object and reconstructs its surface. The surface thus reconstructed has only fixed topological type.

Even though the convolution surfaces provide nice blending between several parts of organs, the control of the blend shape is very limited. The functional representation is a tool that generalize the set theoretic operations and generates full range of shapes from simple object union to smooth blend. The animation of such surfaces follow the changes smoothly, even if the topology changes. Because of this advantage the functional representation become a popular tool where the shapes to be modelled are from the natural world. We explain here our modelling experience that can be useful for others.

2 Convolution Surfaces

In the process of the drawing of special objects, computer graphics algorithms must perform a variety of geometrical calculations. The mathematical representation and manipulation of shapes is, therefore, crucial to the geometric modelling process. Various geometrical representations are used ranging from parametric surfaces through implicit surfaces to solids. The skeleton representation, a standard geometric modelling representation, has become a popular construction tool for implicit design. It consists of an arbitrary number of elements and each element generates an associated implicit primitive.

A parametric surface is given by a special position function $p(u, v) = [x_1(u, v), x_2(u, v), x_3(u, v)]$. In practice, the functions are splines defined by pieces of polynomials, or ratios of polynomials.

An implicit surface is defined by an isosurface of some potential field $F : \mathcal{R}^3 \rightarrow \mathcal{R}$ at threshold level T : $S = \{p \in \mathcal{R}^3 : F(p) - T = 0\}$. The function F is also called an implicit function. A convolution surface is implicitly defined by a potential function F obtained via convolution operator between a kernel and all the points of a skeleton. The convolution surface thus obtained is a smoothed skeleton. The skeleton is a collection of geometric primitives such as point, line segment, arc and plane that outline the structure of an object being modelled. Convolution surface build from complex skeletons can be evaluated individually by adding the local potentials for each primitive, because convolution operator is linear.³ Let us have N

skeleton primitives the above statements can be written as the following modelling equation in an implicit form:

$$\sum_{i=1}^N F_i(x_1, x_2, x_3) - T = 0, \quad (1)$$

where F_i is the source potential of i -th skeleton primitive and T is the iso-potential threshold value.

2.1 Convolution Kernel

Let us have a skeleton primitive represented by a function $p : \mathcal{R}^3 \rightarrow \{0, 1\}$ which is equal to 1 for points belonging to the primitive and 0 otherwise. The total potential at point \mathbf{r} is derived from the convolution operation between function p and a kernel $h : \mathcal{R}^3 \rightarrow \mathcal{R}$. Since p has values 0 or 1 it can be conveniently written as an integral of the kernel function h over the volume V_i of the skeleton primitive:

$$F_i(\mathbf{r}) = \int_{V_i} h(\mathbf{r} - v) dv.$$

McCormack and Sherstyuk^{6,11} define a new kernel that allows analytical calculation of field equation simplified as:

$$F_i(\mathbf{r}) = \int_{V_i} \frac{dv}{1 + s^2 r^2(v)^2},$$

where $r = |\mathbf{p} - \mathbf{r}|$ is the distance from the point to the point in the kernel support and coefficient s controls the width of the kernel, see Fig. 1. The shape

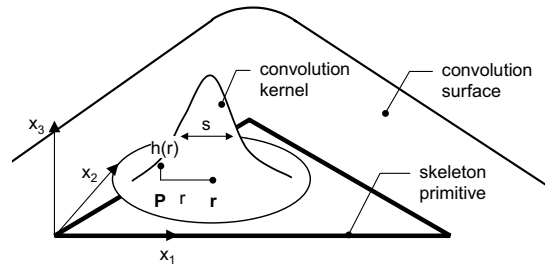


Figure 1. The convolution kernel.

of a convolution surface can be varied in several ways: by changing the skeleton, the changing the convolution kernel, and by spatial deformation of convolution surface.

3 Function Representation

Let us consider closed subsets of n -dimensional Euclidian space E^n with the definition:

$$f(x_1, x_2, \dots, x_n) \geq 0,$$

where f is a real continuous function defined on E^n . The above inequality is called a function representation (F-rep) of a geometric object and function f is called the defining function. In three-dimensional case the boundary of such a geometric object is called implicit surface. The major requirement on the function is to have at least C^0 continuity. The set of points $X_i(x_1, x_2, \dots, x_n) \in E^n$, $i = 0, \dots, N$ associated with Eq. 3 can be classified as follows:

$$\begin{aligned} f(X_i) &> 0 \text{ if } X_i \text{ is inside the object,} \\ f(X_i) &= 0 \text{ if } X_i \text{ is on the boundary of the object,} \\ f(X_i) &< 0 \text{ if } X_i \text{ is outside the object.} \end{aligned}$$

Let us consider from now on the defining function given by the convolution operator between a kernel and all the points of a skeleton, i.e. function F as defined in the last equation of the previous section.

3.1 Set-theoretic Operations

The binary operations on geometric objects represented by functions can be also defined in the form of function representation by

$$\mathcal{F}(f_1(X), f_2(X)) \geq 0, \quad (2)$$

where \mathcal{F} is a continuous real function of two variables.¹⁰ Such operations are closed on the set of function representations. After set theoretic operation between two subjects defined by functions f_1 and f_2 the resulting object has the defining function as follows:

- For object union

$$f_3 = f_1|f_2 \equiv \frac{1}{1+a}(f_1 + f_2 + \sqrt{f_1^2 + f_2^2 - 2af_1f_2}),$$

- for object intersection

$$f_3 = f_1\&f_2 \equiv \frac{1}{1+a}(f_1 + f_2 - \sqrt{f_1^2 + f_2^2 - 2af_1f_2}),$$

- for object subtraction

$$f_3 = f_1 \setminus f_2 \equiv f_1 \& (-f_2),$$

where $|, \&, \setminus$ are notations of so-called R-functions and parameter $a = a(f_1, f_2)$ is the arbitrary continuous function satisfying the conditions

$$\begin{aligned} -1 &< a(f_1, f_2) \leq 1 \\ a(f_1, f_2) &= a(f_2, f_1) = a(-f_1, f_2) = a(f_1, -f_2). \end{aligned}$$

Please, note that even though the resulting defining function for set above theoretic operations is continuous, the resulting object is not continuous in general.

3.2 Blending Union Operation

Intuitively the blending union operation between two initial objects from the set of function representations is a gluing operation. It allows us to control the gluing type in the wide range of shapes from pure set union to convolution like summation of terms. Mathematically the blending union operation is defined by

$$\mathcal{F}(f_1, f_2) = f_1 + f_2 + \sqrt{f_1^2 + f_2^2} + \frac{a_0}{1 + (\frac{f_1}{a_1})^2 + (\frac{f_2}{a_2})^2},$$

where f_1 and f_2 are functions representing objects that are blended. The absolute value a_0 defines the total displacement of the bending surface from two initial surfaces. The values $a_0 > 0$ and $a_1 > 0$ are proportional to the distance between blending surface and the original surface defined by f_1 and f_2 , respectively. The effect of this operation compared to other possible object connections is demonstrated on two object primitives whose skeleton consists of two line segments one vertical and the other one diagonal, see Figure 2 top-left. Simple plus operation between convolution functions deforms the thickness of vertical convolution cylinders as shown in top-right image. Considering four line segments as a single skeleton of geometric primitive results in the shape shown in top-center image. The sequence of shapes shown on bottom of Figure 2 are the blending union operations between two parallel geometric primitives. The geometric primitives and their skeletons do not change but the blending parameters used to blend them are different for each image. In order from left side the used parameters are $a_i = 0.01$, $a_i = 0.07$, $a_i = 0.3$, $a_i = 0.5$, and $a_i = 0.7$, respectively. We can conclude that in the case when the shape and size of geometric primitives must be preserved the blending union operation with different parameters a_0 , a_1 , and a_2 is a good choice. On the other hand when the blending shape is main concern the convolution plus operation should be used. When both the shape of geometric primitives and that of blending are important the small values of blending union parameters is a choice. The F-rep blending union operation has similar advantages as simple convolution union with respect to minimizing unwanted bulges.

4 Organic Models

In previous sections have been discussed the theory of F-rep and convolution surfaces. As next, we will show a method to model the organic shapes by F-rep,

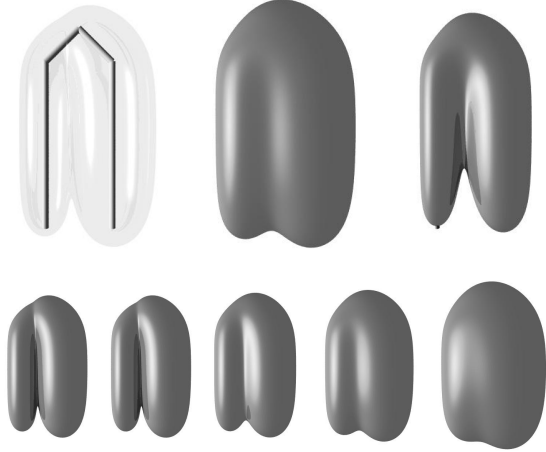


Figure 2. Blending union operation. top: standard and bottom: Blending union operation.

where each of the geometric primitives is defined by

$$\sum_{i=1}^N F_i(x_1, x_2, x_3) - T = 0,$$

where F_i are the source potentials of skeleton primitives i.e. points, lines or triangles and T is a threshold value.

4.1 Model of Stomach

The stomach appears as a fusiform dilation of the foregut in week four of development. Its appearance and position change greatly as a result of the different growth rates of the various regions of its wall, in addition to the position changes of surrounding organs. The liver is the nearest fast-growing organ with large volume. Positional changes are easily explained by assuming that the stomach rotates around a *longitudinal* and an *anteroposterior* axis.

The stomach rotates 90 degrees clockwise around its longitudinal axis. During this rotation, the original posterior wall of the stomach grows faster than the anterior portion, resulting in the formation of the greater or lesser curvatures. During further growth, the stomach rotates around an anteroposterior axis such that the pyloric part moves to the right and upward and the cardiac portion moves to the left and slightly downward.

Several statistical measurements have been made to specify the shape of the stomach growth process. Table 1 shows the mean stomach thickness measured as a radius of a circle perpendicular to the main stomach

day	length [mm]	diameter [mm]		
		c_1	c_2	c_3
21	0.08	0.08	0.08	0.08
28	0.08	0.12	0.21	0.10
35	0.14	0.27	0.34	0.20
70	0.89	3.37	3.55	2.84
84	1.26	5.41	5.71	4.20
140	3.33	14.7	13.3	9.99
252	4.92	25.8	23.4	18.4

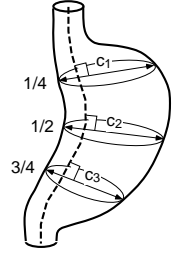


Table 1. Measurements for of human embryo stomach.

axis. Measurements were taken at top, central and bottom locations relative to the length of stomach axis noted as c_1 , c_2 and c_3 .

4.2 F-rep of a Stomach

Since, the topology and the shape of an human embryo stomach is simple a chain of line segments can be used as a skeleton. One may use the spherical representation to obtain the skeleton as shown in Figure 3. Cardiac portion of a stomach is modelled by a branch creating a loop with vertical main skeleton axis. Even in such simple model the mixed use of convolution plus and F-rep blending union comes handy. At the bottom of the branch the convolution plus is applied while near its top the F-rep blending union is used between two geometric primitives corresponding to main and branch axis, respectively, see Fig. 9. The line or curve skeleton

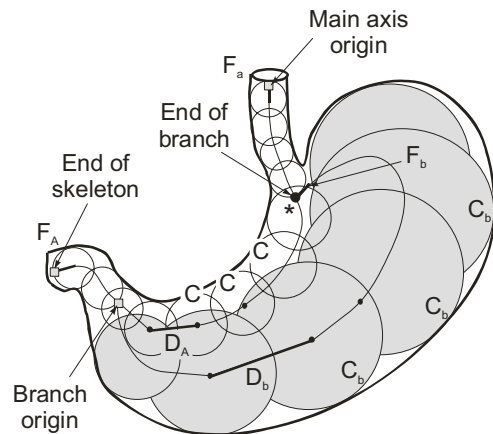


Figure 3. The stomach skeleton of an older stage embryo.

is hard to use when the shape is slightly complicated. As we will demonstrate in this section the human embryo brain needs more complicated skeleton having a 3D tubular form. This extension will give us the ability to model folds or asymmetric bulges.

4.3 Artistic Drawings of Human Brain Development

First step in the model creation process is to obtain the size measurements of brain and stomach stages from atlas of embryology. Embryological atlas contains hand-drawing pictures and photographs of human embryo organs ordered by age. For the purpose of this study the models from 28 - 56 days old brain were used. The brain pictures has been scanned, stored in binary form and measured by ruler. The model, at this stage of precessing, was divided into physiological parts to suite the animation purposes. The outlines of physiological parts were drawn over the pictures and photographs, see Figure 4.

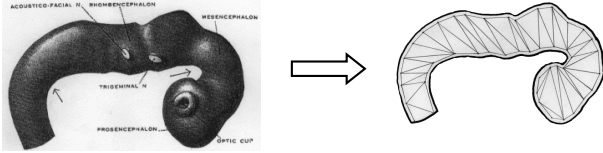


Figure 4. The conversion of drawing human embryo brain to central skeleton.

4.4 Central Skeleton

The result of the measurements is a 2D planar contour, call *the central skeleton*, nearly outlining the outer contour of the shape. Interior of central skeleton is triangulated such that it crates a triangular strip. One can observe different growth speed for different pars of embryo brain. It is therefore natural to divide the central skeleton into those parts. Additional parts could be necessary to model the folds and control the unwanted blending problem near the folding areas. Figure 5, shows namely the part I corresponding to the part of brain called rhombencephalon, part II will develop to mesencephalon and part III is a prosencephalon. The next step is to calculate the central line that will be used as a base to define the thickness of the model along the line forming the tubular object. Central line passes through the center of central skeleton, connecting the mid points of vertical edges of a triangular strip.

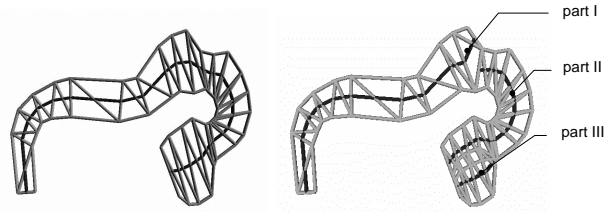


Figure 5. Dividing the central skeleton to 3 parts. The line in the middle of the central skeleton is called central line.

4.5 Skeleton

By adding the thickness to 2D central skeleton the 3D skeleton of the model is obtained. Multiple number of copies of central skeleton are slightly scaled and shifted to left and right sides of central skeleton. By this way the cross sections are produced which are then connected to form the tubular skeleton, see Figure 6:

- Each of side skeletons is scaled to fit the ellipses whose center is on the central line. Radius a of the ellipse is a distance to the central line from the border of the central skeleton. Radius b follows the equation, $b = \alpha a$, where α is a ratio parameter.
- As next step, for a given θ the side skeletons are translated by distance $t = c \cos \theta$, where c is known from parametric equation of ellipse shown in Figure 7.
- Finally, side skeletons are connected with a central skeleton or with other side skeletons by a triangular mesh.
- After erasing all interior triangular patches we obtain multiple tubular shapes forming together the entire skeleton of the brain.

5 HyperFun Modeling

A smooth convolution surface defined over the triangular mesh of tubular skeleton creates the model of embryo brain. In order to create brain model with convolution surfaces, we use HyperFun^{1,9} as modelling library and POV-Ray⁸ as rendering software. HyperFun command hfConvTriangle generates convolution surface over the triangles which suites our problem. Let us discuss all parameter settings for one particular example, the *stage3* human embryo brain shown in Figure 8. The convolution kernel width is set to

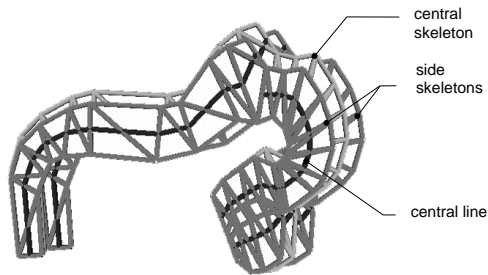


Figure 6. Adding the thickness by scaling and shifting the central skeleton.

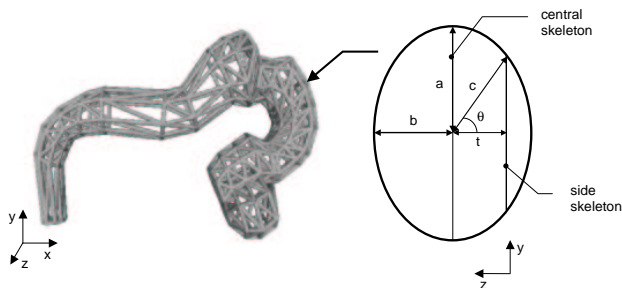


Figure 7. A 3D skeleton for 36 days old human embryo brain.

$s = 0.5$ and iso-potential threshold value is $T = 0.6$. The ration parameters of brain thickness have been set to $\alpha = 1.0$ at parts I and II and to $\alpha = 1.2$ at part III. Nice blending during the animation can be guaranteed by blend-union operation between three parts of this model using the HyperFun command hfBlendUni. The blending parameters $a_1 = a_2 = a_3 = 0.2$ are used for both gluing parts I, II and parts II and III, respectively.

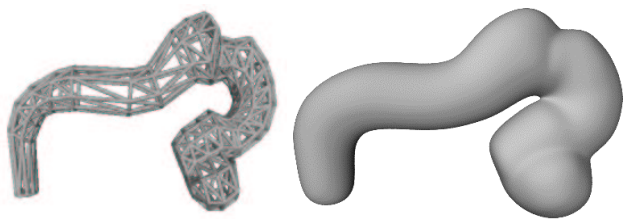


Figure 8. Stage3 human embryo brain. Left: 3D tubular skeleton, right: entire brain model, defined by function representation.

Stages	Age [days]	Size (mm) [mm]	Number of	
			skeleton triangles	parts
Stage1	28	3.5	296	1
Stage2	32	5	476	1
Stage3	36	9	588	3
Stage4	42	11	548	3
Stage5	49	15	724	4
Stage6	56	27	704	4
Stage6	72	56	710	4

Table 2. Model data.

6 Animation

The good key-frame models and correct morphing interpolation between them are necessary for implicit surface animations. The embryological atlas consists of 8 artistic drawings of the human embryo brain development. We have used first 7 images as key-frame models for the animation process. The key-frame models named Stage1,..., Stage7 have their basic measurements and statistical information collected in Table 2.

6.1 Morphing

The shape transformations can be applied to the various types of graphical objects, such as 2D drawings, images, surfaces and volumes. Given a certain specification, there are various choices in implementing the transformation, not only in selecting the type of modeling, but also in deciding how the object data will be transformed. There does not exist a general morphing technique we could use in our case because the available techniques use strictly the shape and topology information but they neglect the known growth processes, movements and knowledge of embryologists. A work described in⁵ proposed a skeleton feature vectors but they still use a blending technique to hide the topology errors that occur during their 3D morphing step. We decided to propose the featured-based 3D morphing technique with a simple user interaction to control the complicated growth process. Our technique uses both the global deformations to roughly match the global movements of the brain during the growth and the local morphing technique to correct the shape details. To generate the models between key-frame brain stages we used various types of interpolation. Metamorphosis from Stage1 to Stage2, Stage2 to Stage4 and from Stage4 to Stage7 uses the tricubic interpolation based on Catmull-Rom interpolating curves. The Catmull-Rom splines for one-dimensional case, can be

expressed by the following matrix formula⁴:

$$C(u) = UMP^T, \quad (3)$$

where $U = [u^3, u^2, u, 1]$, $P = [p_{i-1}, p_i, p_{i+1}, p_{i+2}]$, and

$$M = \begin{bmatrix} -0.5 & 1.5 & -1.5 & 0.5 \\ 1.0 & -2.5 & 2.0 & -0.5 \\ -0.5 & 0 & 0.5 & 0 \\ 0 & 1 & 0 & 0 \end{bmatrix}.$$

$C(u)$ is the interpolated value, $p_{i-1}, p_i, p_{i+1}, p_{i+2}$ are four consecutive data points and $u \in [0, 1]$ is a parameter that defines the fractional position between p_i and p_{i+1} .

Catmull-Rom interpolation is used to interpolate position between skeleton points, values of convolution filter parameters s and T , thickness parameters α, θ and the blending parameters a_0, a_1 and a_2 . This technique generates good in-between models. The spline technique can move vertices of existing skeletal triangles, but it can also generate intermediate skeletons by splitting or merging the vertices of existing triangles. Even though the skeleton change is discrete the convolution surface changes smoothly because of linear property of convolution operator. Similarly when the number of skeleton parts is different a new part is created from a single vertex on the tubular skeleton. As a result we have no visually objective jumps during skeleton based growth animation.

The visual result of modeling human embryo brain using function representation is an animation. The number of in-between key-frame models depended on the age of key-frame models. We generated 10 in-between frames for one day of development. One second in the final animation corresponds to 3 days of human embryo development.

Direct ray-tracing of our convolution surface models took about three weeks on PIII 700MHz, much faster approach is to polygonize the convolution surfaces and then ray-trace them in the complex lighting scene, taking approximately 4 hours. Few frames from animation of *Organ growth* show the embryo stomach and brain described by embryo age and the real size scale bar, see Figures 9, 10.

7 Conclusions

We succeeded to model virtual human embryo organs, namely stomach and brain using convolution surfaces and functional representation. The growth animation of a stomach was generated for all 9 months of development while the brain growth animation was generated for first 4 months of embryo development.

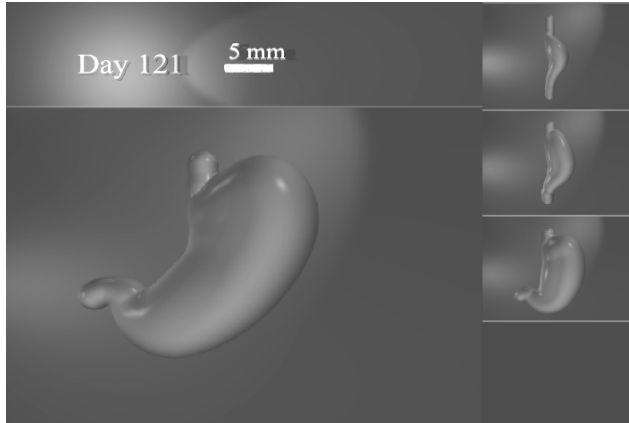


Figure 9. A single frame from the human embryo stomach animation.

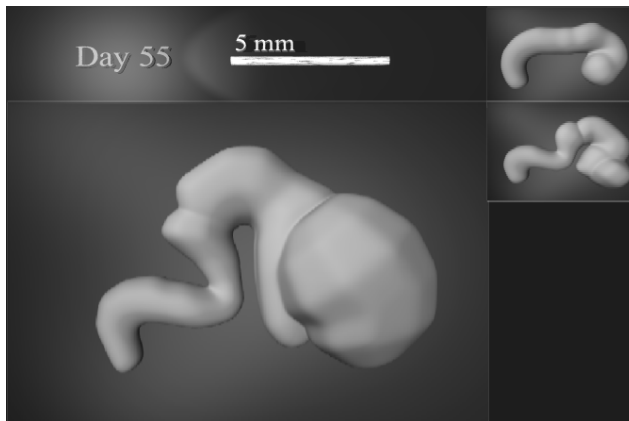


Figure 10. A single frame from the human embryo brain animation.

The advantage of skeleton based approach is that it avoids the topology artifacts that can occur when using the nonlinear interpolation between two defining functions of F-rep models. Variable speed of growth and shape thickness is successfully modelled by convolution plus or blending union between model parts. This is also a solution to unwanted blending problems. The method produces smooth shape changes although the changes of tubular skeleton geometry are discontinuous when new vertices or triangles are created.

In the future work we implement branches and details for brain models and create grown-up brain models and growth animation between older human embryos. The same approaches can be used for other human organs. The future plan is to show the growth of intestinal system combined with other large organs.

Acknowledgements

Authors wishes to thank Mineo Yasuda from Medical School of Hiroshima University for sharing the knowledge as an embryologist. The images were rendered by the POV-Ray ray-tracing program programmed by POV-Ray Team. This research was sponsored by grants from the Fukushima Prefectural Foundation in Japan for the Advancement of Science and Education.

References

1. V. Adzhiev, R. Cartwright, E. Fausett, A. Ossipov, A. Pasko, V. Savchenko HyperFun project: A framework for collaborative multidimensional F-rep modeling, *Implicit Surfaces '99, Eurographics/ACM SIGGRAPH Workshop*, J. Hughes and C. Schlick (Eds.), Bordeaux, France, September 13-15 1999; 59-69.
2. D. Attali, A. Montanvert, *Semi-continuous skeletons of 2D and 3D shapes in C*. World Scientific, 1994.
3. J. Boolmethyl, K. Shoemake, Convolution Surfaces, *Proceedings of SIGGRAPH'91*, Las Vegas, NV, in Computer Graphics 25, 4, July 1991.
4. J. Foley, A. van Dam, S. Feiner, J. Hughes, *Computer graphics principles and practise*, Second edition in C. Addison-Wesley, Reading, Massachusetts, 1997.
5. A. Leros, C. Garfinkle, M. Levoy, *Feature-based volume metamorphosis*, 449-456.
6. J. McCormack and A. Sherstyuk, Creating and Rendering Convolution Surfaces, *COMPUTER GRAPHICS forum*, no. 2, 1998; 17: 113-120.
7. S. Muraki, *Volumetric shape description of range data using blobby model*. In Computer Graphics (SIG-Graph '91 Proceedings), Las Vegas, NV, 1991, 227-235.
8. WEB page. POV-Ray - the Persistence of Vision Raytracer -, <http://www.povray.org>, January 2001.
9. WEB page. Shape modeling and computer graphics with real functions, in <http://wwwcis.k.hosei.ac.jp/F-rep/F-rep.html>, January 2001.
10. A. Pasko, V. Adzhiev, A. Sourin, V. Savchenko, Function representation in geometric modeling: concepts, implementation and applications, *The Visual Computer*, No. 8, 1995; 11: 429-446.
11. A. Sherstyuk, Interactive Shape Design with Convolution Surface, *Proceedings of Shape Modeling and Applications*, Aizu-Wakamatsu, Japan, 1999, 56-65.
12. N. Tsingos, E. Bittar, M. Gascuel, *Implicit surfaces for semi-automatic medical organ reconstruction*. in Computer Graphics: Developments in Virtual Environments (Proceedings of Computer Graphics International '95), UK, 1995, 3-15.
13. R. Đurikovič, K. Kaneda and H. Yamashita, Imaging and modeling from serial microscopic sections for the study of anatomy. *Medical and Biological Engineering and Computing* Nov. 1998; 36: 276-284.